J. Earth Syst. Sci. (2021)130 154
https://doi.org/10.1007/s12040-021-01652-9

Paleointensity of the Earth's magnetic field at ∼117 Ma determined from the Rajmahal and Sylhet Trap Basalts, India

M R Kapawar and Venkateshwarlu Mamilla*

CSIR-National Geophysical Research Institute, Hyderabad, India.
**Corresponding author. e-mail: mamila_v@rediffmail.com*

MS received 5 December 2020; revised 26 January 2021; accepted 30 March 2021

We present here the paleointensity results of basalt samples from Rajmahal (25.10°N; 87.40°E) and Sylhet Traps (25.22°N; 91.71°E) of eastern India (∼117 Ma) to know the strength of the earth's magnetic field during the early Cretaceous from these locations. The modified version of the Thellier–Thellier paleointensity method of, in field-zero field-zero field-in field (IZZI) protocol and systematic partial thermoremanent magnetization (pTRM) checks were used for the paleointensity determination. Rock magnetic investigations on these rocks indicate 'magnetite' is the main remanence carrier with single domain (SD) to pseudosingle domain (PSD) nature. The samples have yielded low paleofield intensities between 6.97 ± 2.21 and 23.47 ± 2.08 μT (mean 17.20 ± 1.89 μT). The corresponding virtual dipole moment (VDM) ranges from 1.16 to 4.17 × 10^{22} Am^2 (mean 2.93 × 10^{22} Am^2) which is approximated as to 30% of the present-day field strength (8 × 10^{22} Am^2). The success rate of the experiment is quite low in the order of 5%, but has provided scope for further, more elaborative paleointensity studies. Our new results compared with published paleointensities from these basalts as well as rocks of Cretaceous normal superchron (CNS) time around the globe are in good agreement.

Keywords. Paleointensity; IZZI protocol; early Cretaceous; Rajmahal–Sylhet Traps; India.

1. Introduction

The earth's magnetic field is generated within the fluid outer core and convective motion takes place within the earth's mantle by a self-exciting geodynamo (e.g., Glatzmaier *et al.* 1999). The analysis and description of the direction and strength of earth's magnetic field through the geologic past reveals information about the history and its development. Variation in paleointensity over geologic time may indicate modulation of geodynamo in the core by the convective motion of the lower mantle (Goguitchaichvili *et al.* 2002) and its interaction with the liquid outer core. As per Coe *et al.* (2000), an estimation of absolute intensity should be a basic approach in numerical models that provide unknown insights into the geodynamo operation. The available paleointensity data remain insufficient (Selkin and Tauxe 2000), and thus cannot be used for reporting a long-term variation in the intensity of the earth's magnetic field.

The paleomagnetism yields better results in terms of the directional component of earth's magnetic field, but the earth's magnetic field variation not only occurs in direction but also in its strength. The paleointensity data on geomagnetic field strength is very precious to document the

Published online: 02 August 2021

behaviour and variations of earth's magnetic field during key periods, like the early Cretaceous. Well-documented directional records are available for this period but the prominent paleointensity results are still not well documented. Few studies of Cretaceous (Loper and MacCartney 1986; Prevot *et al.* 1990; Pick and Tauxe 1993; Tanaka *et al.* 1995; Perrin and Shcherbakov 1997; Radhakrishna *et al.* 2020) suggested the low-field strengths during the Cretaceous normal superchron (CNS); however, studies (e.g., Tarduno *et al.* 2001, 2002; Tarduno and Smirnov 2001; Tauxe and Staudigel 2004) reported high field values. Such a discrepancy between the various studies from rocks of single polarity could be due to the type of material used for the experiments and magneto-mineralogical alterations during the experiment. Therefore, further studies are essential to better define and understand the time-averaging properties of earth's magnetic field and its thermal history.

The Indian Plate has the Rajmahal–Bengal–Sylhet (RBS) volcanic province that belongs to an early Cretaceous time and represents the initial phase of volcanism associated with the Kerguelen hotspot (mantle plume). This also marks the breakup of eastern Gondwana configuration, i.e., the break-up of Indian Plate from the Australia–Antarctica Plates (Baksi *et al.* 1987; Kent *et al.* 2002; Coffin *et al.* 2002). The paleomagnetism of RT basalts has yielded vast information about the paleodirection of the geomagnetic field than about the paleointensity. It is noted that only two reliable paleofield strength reports from Rajmahal Traps (RT) (Sherwood *et al.* 1993; Tarduno *et al.* 2001) and not a single from Sylhet Traps (ST) are available. These studies have reported a virtual dipole moment (VDM) of $5.5 \pm 1.9 \times 10^{22}$ Am^2 (Sherwood *et al.* 1993) and $12.5 \pm 1.4 \times 10^{22}$ Am^2 (Tarduno *et al.* 2001). The prime reason behind very few attempts could be that the paleointensity is a difficult element of the earth's magnetic field to estimate, the success rate of paleointensity experiments are usually very low of the order of 10%, and the prolonged nature of the paleointensity experiments.

These discrepancies in paleointensity studies conducted for RBS province has offered us a scope for the present study and considering its importance towards global paleointensity dataset, the paleointensity and rock magnetic analyses were performed on early Cretaceous basalts belonging to RT and ST of India. The varying earth's magnetic field strengths during the CNS, especially during the early Cretaceous have been examined.

2. Geologic setting and sampling

The geologic and geodynamic research associated with flood basalt provinces has identified the presence of mainly two flood basalt provinces over the Indian Plate, one is Deccan Traps on the western margin of India and another is the Rajmahal–Bengal–Sylhet (RBS) Traps on the eastern margin. Of these, the present study focuses on the basalts of RT and ST of ∼117 Ma, attributed to the Kerguelen hotspot. The RT is exposed over mainland India, mainly in the Jharkhand state, while the ST is exposed at the southern margin of the Shillong Plateau of Meghalaya, northeast India. It seems that although both have similar age of formation, placed at a distance from each other, for which Evans (1964) has explained the plausible reason as, the movement of Shillong Plateau by ∼250 km eastward along the Dauki Fault. The total areal extent of the RBS volcanic province is believed to be $\sim 2 \times 10^5$ km^2 (Baksi 1995). These are situated ∼450 km apart and the area between them is covered by Cenozoic alluvium carried by Brahmaputra and Ganga Rivers.

The lava flows of RT basalts have an areal extent of ∼4500 km^2 and exposed between 24°05′–25°15′N latitude and 87°24′–87°51′E longitude. Similarly, ST is exposed in the form of a narrow strip of ∼80 km long and 5–6 km wide E–W band (∼240 km^2) having a thickness of ∼550–600 m (Sarkar *et al.* 1996). The exposed thickness of the ST is ∼300 m (Ray *et al.* 2005), which is greater than the exposed thickness of the RT (∼230 m; Kent *et al.* 2002; Ghatak and Basu 2013). The ^{40}Ar–^{39}Ar ages of 118–115 Ma (Kent *et al.* 2002; Ray *et al.* 2005) and normal polarity of basalts of RT and ST (Kapawar and Venkateshwarlu 2019, 2020) suggest that they are analogous to the longer C34 normal magnetic polarity chron. Ray *et al.* (2005) have also quoted the genetic relation of the ST with the RT and the parental Kerguelen plume. Both RT and ST are dominantly tholeiitic basalts. Stratigraphically, the RT Formation overlie the older Dubrajpur Formation comprising sandstones and shales, while ST overlies the eroded Precambrian basement complex, and is in turn overlain by Cretaceous sandstones of Shillong Plateau (Talukdar and Murthy 1971).

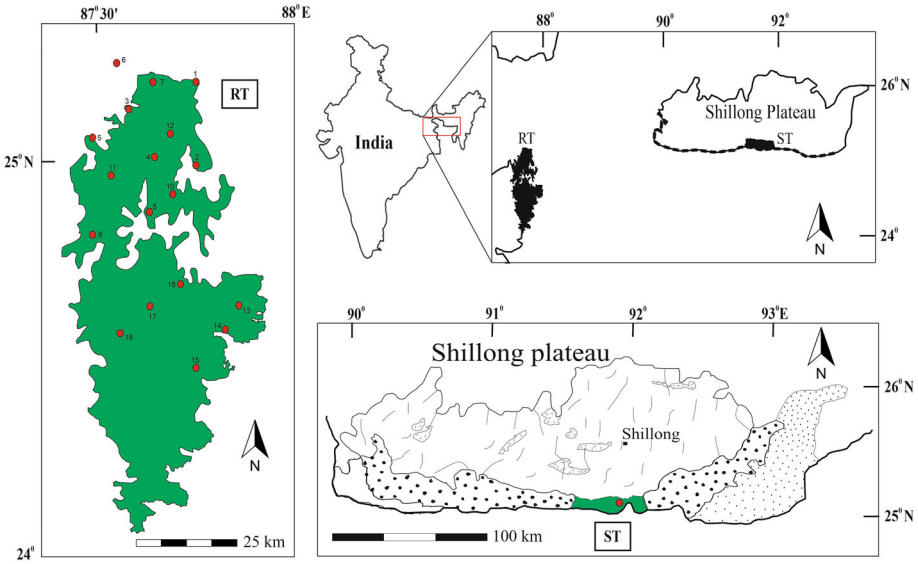

Figure 1. The sketch map showing the exposures of Rajmahal Traps (RT) and Sylhet Traps (ST). Red dots are sampling locations.

The sampling locations of both RT and ST are presented in figure 1. The RT is comparatively more accessible and available for sampling than ST, where most ST exposures are covered under thick vegetation and along the steep hill slopes. The best exposures for ST are along the Cherrapunjee–Shella bazaar road transect and Mawsynram–Balat transect. One hundred and thirty block samples from both RT and ST were collected from quarries and road cuttings. Of which 97 sister samples of RT and ST were selected for the PI study based on the paleomagnetic and rock magnetic results by Kapawar and Venkateshwarlu (2019, 2020). Such selected sister samples were remeasured here to find the rock magnetic consistencies within sister samples.

3. Laboratory experiments

Knowledge of rock magnetic properties stand significant in performing the PI study and serves as a top-grade selection criterion that could provide reliable PI measures. In this study, the rock magnetic properties including hysteresis loops and thermomagnetic curves were conducted to identify the magnetic mineralogy, thermomagnetic stability, mineral grain sizes, and their domain states, using an advanced variable field translation balance (AVFTB). The powdered samples weighing around 400–600 mg were used for 40 representative samples from 26 sites covering both RT and ST.

The PI experiment intervals followed the IZZI (in field-zero field-zero field-in field) protocol (Tauxe and Staudigel 2004; Yu *et al.* 2004; Yu and Tauxe 2005), of the modified double-heating method of Thellier (Thellier and Thellier 1959) including partial thermoremanent magnetization (pTRM) checks for identifying the magneto-mineralogic alterations caused by heating (Prevot *et al.* 1985). The IZZI protocol has an advantage over other methods in terms of remanence stability (Yu and Tauxe 2005). For this, a total of 97 specimens (79 of RT and 18 of ST) were selected and subjected to the PI experiments. A laboratory field of 30 mT was applied during in-field steps and involves a total of 33 temperature intervals including one NRM and six pTRM checks. The initial temperature step was 100°C and progressively increased by 50° till 450°C. Later the temperature intervals were increased by 30°C till the last interval of 600°C. The six pTRM intervals incorporated were at 100°, 200°, 300°, 400°, 480°, and 540°C.

The heating treatment was performed using the MMTD-80 thermal demagnetizer (Magnetic Measurements, UK) and the remanence was measured using AGICO's JR6 spinner magnetometer (Czech Republic). The additional susceptibility measurements were performed after each remanence measurement using AGICO's MFK1-FA susceptibility apparatus (Czech Republic) for better watch over the magnetic stability of the experiment. All the rock magnetic and PI measurements were carried out at the Paleomagnetism Laboratory,

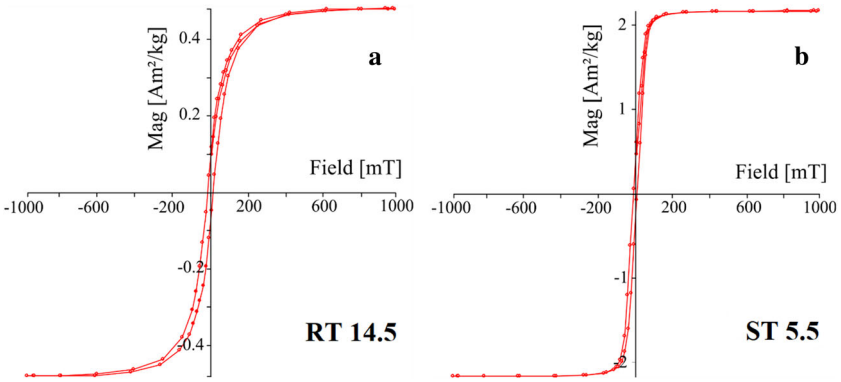

Figure 2. Examples of hysteresis curves after paramagnetic corrections.

CSIR-National Geophysical Research Institute (NGRI), Hyderabad, India.

4. Results

4.1 *Rock magnetism*

The representative magnetic hysteresis loops obtained for these samples depict only two types of behaviour that are subtracted for paramagnetic contributions and presented in figure 2. The maximum applied field is 1 Tesla. From the hysteresis loops the parameters, including saturation remanent magnetization (Mrs), saturation magnetization (Ms), coercivity remanence (Hcr), and coercive force (Hc) were determined using RockMagAnalyzer 1.0 software (Leonhardt 2006). Further, the remanence ratio (Mrs/Ms) and coercivity ratio (Hcr/Hc) were calculated for understanding the domain states and the Day plot (Day *et al.* 1977) is prepared with theoretical mixing lines for magnetite (Dunlop 2002a, b) as shown in figure 3. The results reveal that the majority of recorded remanence was carried by magnetic grains falling in the pseudosingle domain (PSD) region for ST and single domain (SD) for RT. It is understood that samples with SD or sometimes PSD nature, considered good for PI estimation.

In figure 2, the hysteresis curve lines appear to have a thin (closed-loop) nature, indicating fine-to-medium magnetic grain size of samples. Sample RT 14.5 has attained magnetization saturation at ∼400 mT (figure 2a), whereas sample ST 5.5 under 200 mT (figure 2b). It suggests the predominance of low coercive magnetic minerals in samples from both the RT and ST.

The Day plot (figure 3) depicts that RT samples belong to SD state and ST samples belong to

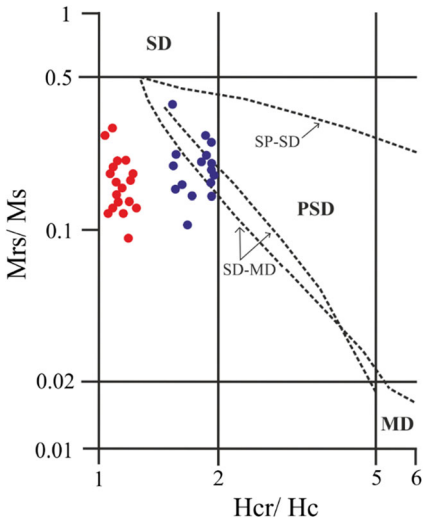

Figure 3. The Day plot (Day *et al.* 1977) is where, Mrs/Ms (remanence ratio) is taken as a function of Hcr/Hc (coercivity ratio), distinguishes between domain states of magnetic minerals in samples. The fields of single domain (SD), pseudosingle domain (PSD), and multidomain (MD) are given with theoretical SD-MD and SP-SD mixing lines (Dunlop 2002a, b) shown as dashed lines. The red (blue) dots belong to RT (ST) samples, show distinct individual grouping.

majority of SD and a smaller extent to PSD. The main magnetic mineral identified is magnetite in both RT and ST. The accessory minerals like low Ti-titanomagnetite, ilmenite, pyrrhotite, and maghemite from the Titanomagnetite Solid Solution (TMS) series are reported (Kapawar and Venkateshwarlu 2019, 2020) from these rocks.

The examples of thermomagnetic curves from both RT and ST are given in figure 4. The thermomagnetic curve is to get the Curie temperature (Tc) and was determined by an intersecting tangent method which is the maximum gradient in the heating curve. In this, each sample was subjected to heating up to a maximum temperature of 700°C and again cooled back to room temperature. The samples from RT (RT1.2;

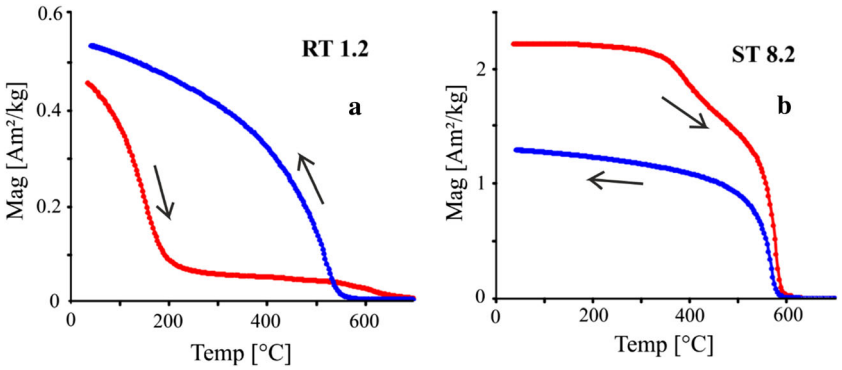

Figure 4. Examples of thermomagnetic curves. The red (blue) lines represent the heating (cooling) cycles with arrows indicating experiment progression, heating followed by cooling.

figure 4a) show a considerable susceptibility loss in the heating cycle near ∼200°C indicating the presence of ilmenite and becomes zero after 600°C. This higher Tc surpassing 600°C, indicating the presence of a minor proportion of haematite or small scale oxidized magnetite, evident of partial thermal alteration in samples. The cooling cycle for RT1.2 starts near ∼575°C and no signs of magnetic susceptibility fluctuations suggest the presence of a stable magnetic phase, that corresponds to magnetite. The thermomagnetic curve of the ST samples (ST8.2; figure 4b) produces a minor susceptibility loss between a temperature interval ∼380–450°C and later goes to zero at ∼580°C.

The low Tc component likely corresponds to low Ti-titanomagnetite that altered to higher Tc component magnetite. The cooling cycle of this sample does not indicate low Ti-titanomagnetite, but the pure magnetite depicting its complete transformation after heating. Both these thermomagnetic curves possess dual magnetic components and the heating cycles are thermally unstable than cooling cycles, suggesting their irreversible nature. Furthermore, this rock magnetic supplementary information for basalts from RT and ST can be utilized for a better PI estimation in this study.

4.2 *Paleointensity*

The results are presented on an Arai plot (Nagata *et al.* 1963), in which the natural remanent magnetization (NRM) remaining after the zero-field step is a function of respective pTRM gained in the laboratory field for successive temperature intervals. Ideally, the ratio of the NRM lost to the pTRM gained remains constant throughout the entire temperature interval. The experimental results are presented in figure 5, which has examples of Arai plots, intensity decay curves, Zijderveld plots, and susceptibility monitoring curves for the samples that yielded the reliable PI estimations. The data points are represented by an open circle that includes both IZ and ZI intervals forming a single straight line on the Arai plot. The pTRM checks with triangles are also denoted. The slopping of this line, where the ChRM is attained by sample on the Arai plots, is used in the estimation of the PI values. Almost all the specimens revealed the presence of more than one magnetic component and suggested a severe amount of thermochemical alterations.

Very few samples passed the selection criteria for reliable estimation of PI, and results are presented in table 1 and figure 5. It is necessary to discuss the selection criterion considered for PI estimations before going to detailed results, and are listed as below:

(1) The use of more than seven successive data points (N).
(2) The linear fit standard deviation (std) should be less than 0.15.
(3) The directional alpha (α) criteria should be less than 10°.
(4) The directional maximum angular deviation (MAD; Kirschvink 1980) criteria of the data points on an orthogonal plot should be less than 10°.
(5) The linear fit criteria of the fraction of the NRM (f) should be more than or equal to 0.3.
(6) The important linear fit criteria that decide the reliability of PI estimation, the quality factor (q) should be more than 1.

These criteria are as discussed in ThellierTool4.1 by Leonhardt *et al.* (2004). Satisfying these criteria, only four specimens out of 97 have yielded successful results with a very low success rate (<5%).

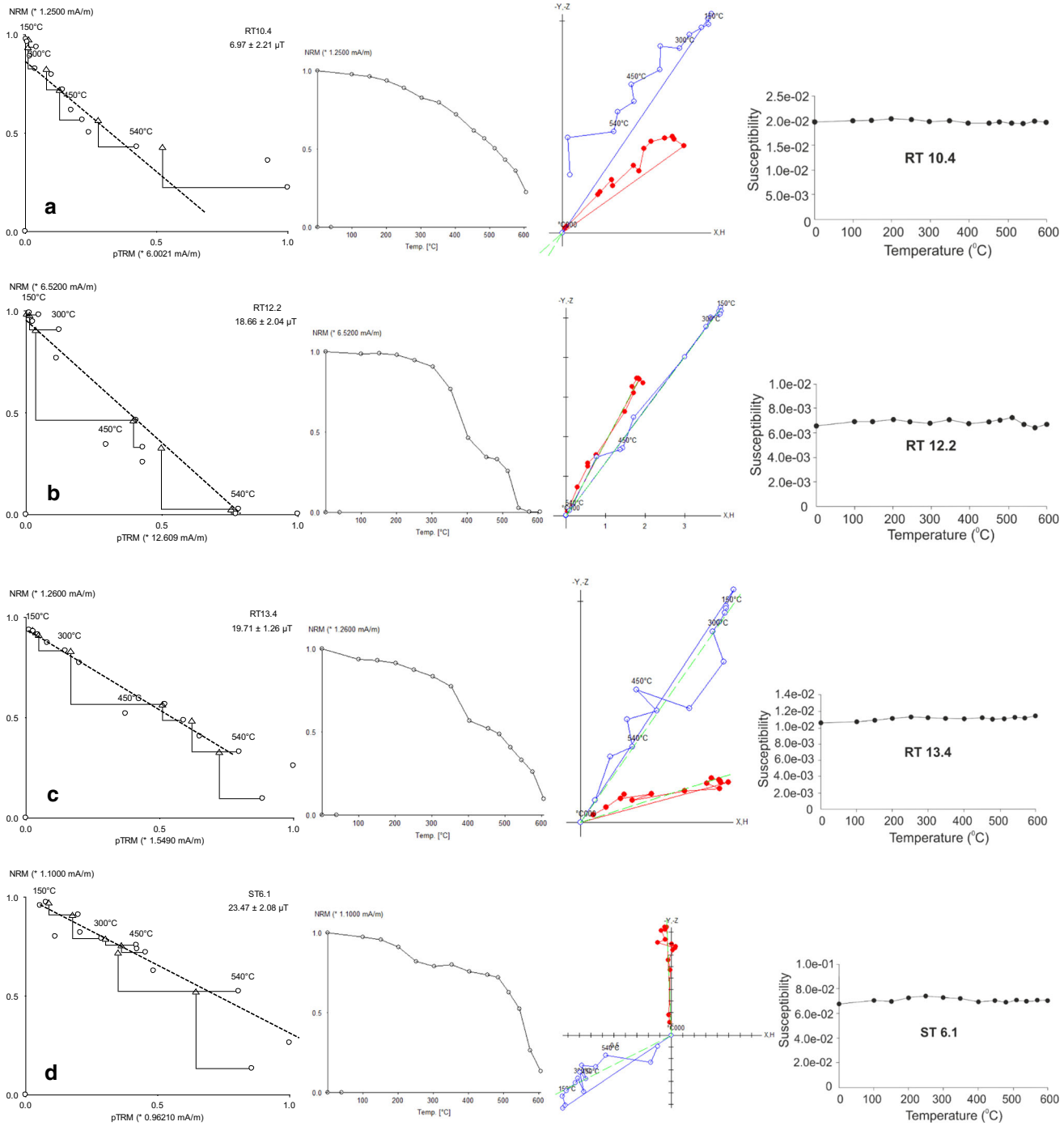

Figure 5. The representative Arai plot, intensity decay curve, Zijderveld plot, and the susceptibility monitoring curve generated from the paleointensity data of accepted **(a, b, c, d)** and rejected (**e** and **f**) specimens.

An average percentage change in susceptibility during paleointensity experiment for accepted specimens <7% suggests partial or no alteration, while those rejected are having a change in susceptibility between 20 and 25%. Most of the rejected samples have suggested one or two indications of alterations, but confirms severe thermochemical alteration with progressive and repetitive heating. The mean paleointensity calculated from the accepted specimens is 17.20 ± 1.89 µT that corresponds to the mean VDM of 2.93×10^{22} Am^2.

5. Discussion

5.1 *Data reliability and literature comparison*

Early Cretaceous time preserves vital earth's magnetic field variations from a stage of

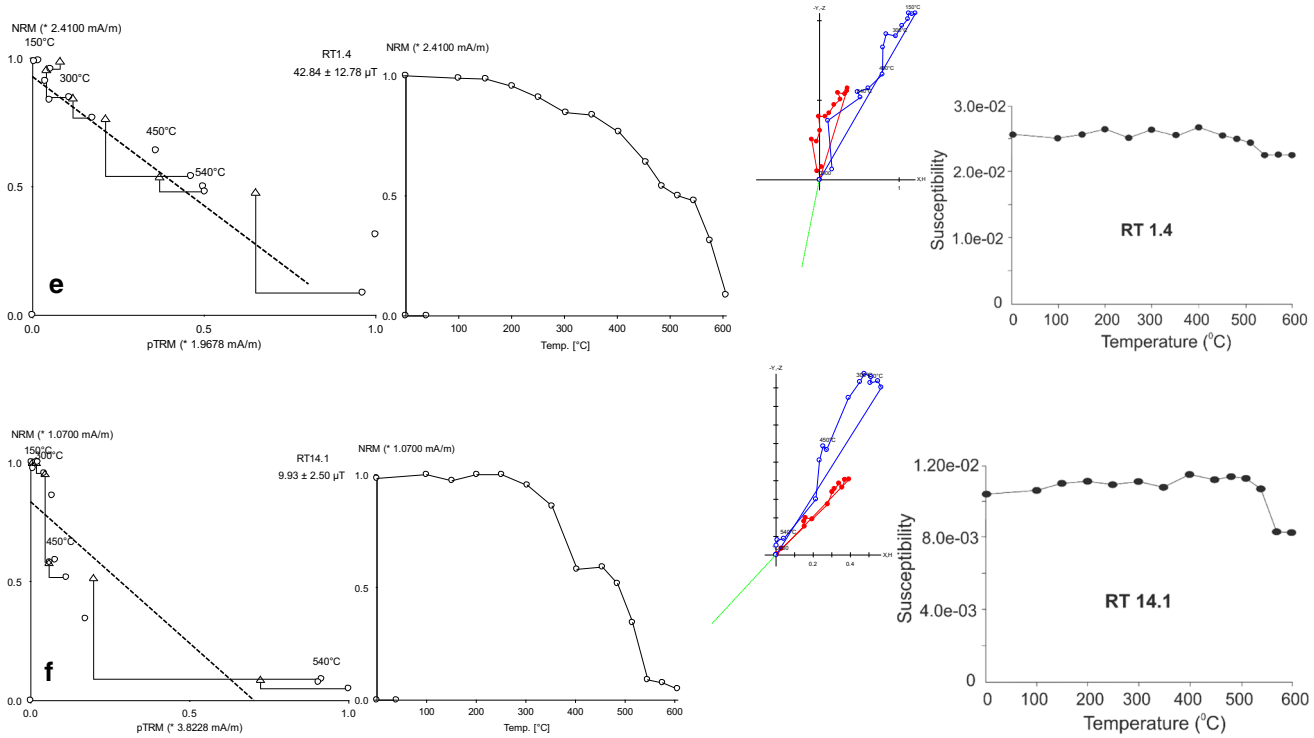

Figure 5. (*Continued.*)

Table 1. *Representative paleointensity estimations from basalts of RT and ST with four reliable results.*

Sample	T (°C) range	N	Std	α	MAD	f	q	F (μT)	VDM × 10^{22} Am^2
RT1.4	0–570	13	0.29	3.90	4.33	0.87	1.24	34.90 ± 8.56	5.81
RT7.3	100–550	10	0.24	2.07	3.31	0.94	2.82	16.72 ± 4.15	2.79
RT10.4*	0–570	13	0.13	4.98	5.07	0.89	1.28	6.97 ± 2.21	1.16
RT12.2*	100–570	12	0.10	0.73	7.57	1	6.76	18.66 ± 2.04	3.11
RT13.4*	100–540	11	0.06	5.42	4.79	0.65	7.98	19.71 ± 1.26	3.28
RT14.1	100–570	12	0.21	0.79	2.54	1	3.43	8.85 ± 1.55	1.47
RT18.2	0–570	13	0.25	3.10	9.30	1	1.34	2.20 ± 0.56	3.66
ST3.3	0–550	11	0.26	5.09	7.66	1	3.14	43.22 ± 11.31	7.68
ST5.4	0–570	13	0.28	0.80	3.88	1	1.32	10.77 ± 3.10	1.91
ST6.1*	100–570	12	0.08	2.00	6.03	0.67	5.95	23.47 ± 2.08	4.17

T (°C) range is the temperature range used on the Arai plot for PI determination; F is the paleointensity estimate for the individual specimen; VDM is the virtual dipole moment for studied location. * represents accepted specimens based on the criterion described above, respective Arai plots, and lesser percentage change in susceptibility.

fluctuations in the magnetic polarity to the longer and stable normal polarity chron (C34) for around 40 Ma. The Indian Plate has rocks that belong to the C34 chron and are basalts of RT and ST aging ∼117 Ma. The PI study was performed here, and estimated the values of VDM. Many data reliability measures were taken before the results were considered as accepted. This reliability assessment is due to the rock magnetic analyses and room temperature susceptibility measurements. This includes the hysteresis properties, thermomagnetic analyses, pTRM checks, and changes to the magnetic susceptibility during the experiments. The major barrier in obtaining the reliable PI results is magnetic mineral alterations and secondary overprinting that masks the primary remanence. In this

study to obtain PI results from magnetic minerals only SD-PSD magnetic grain sizes are used which are usually suitable for the study of earth's magnetic field strength. Most of the samples from ST and RT are unlikely to present reliable PI values although they carry SD-PSD grain size, still, few of the samples have qualified and presented reliable value. After qualifying all the concerned criteria, the accepted sample data seems reliable for its further usage like, to comment about the earth's magnetic field strength at the beginning of CNS and fluctuations (if any).

The PINT database (Biggin and Paterson 2014) was used for the comparison of the data for both, from RT and studies of similar-aged rocks spanning between 110 and 120 Ma. This comparison of the present mean value obtained in this study with literature reports (figure 6), support a low field strength (Pick and Tauxe 1993; Sherwood *et al.* 1993; Sakai *et al.* 1997; Zhu *et al.* 2001, 2003, 2004; Goguitchaichvili *et al.* 2002, 2008; Pan *et al.* 2004; Tauxe 2006; Qin *et al.* 2011; Mena *et al.* 2011). A study performed over RT by Tarduno *et al.* (2001) has reported higher field strength during this period, and our study results disagree with it. This reported high field strength value could be due to transitional magnetic field. Although the methods adopted were same, the justification for disagreement between results of the present and literature study (i.e., Tarduno *et al.* 2001) lies in the sample material used. In the present study, we used whole-rock samples for PI estimations whereas Tarduno *et al.* (2001) used single plagioclase crystals derived from the whole rock samples. To be noted that, whenever single plagioclase crystals were used for PI estimations, it has yielded higher PI values (Tarduno *et al.* 2007; Kato *et al.* 2018) than whole-rock samples and generally does not agree with the anticipated low field strength and that of available datasets for the early Cretaceous time. Cottrell and Tarduno (2000) considered the usage of single plagioclase crystals but also agreed on the usefulness of whole-rock samples for PI estimations. The obtained results from whole-rock basalts in the present study are in good agreement with the theoretical values in literature (figure 6) suggesting low-field strength during early Cretaceous.

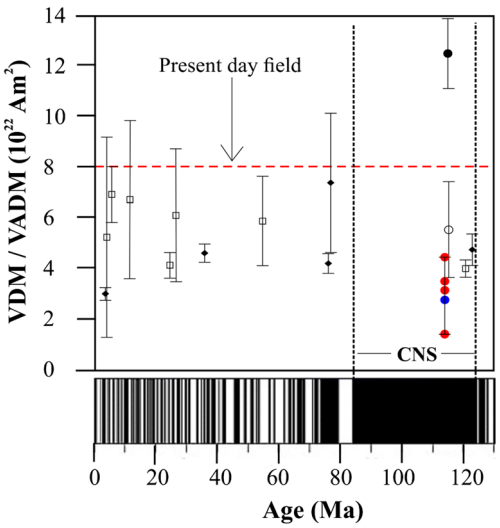

Figure 6. Virtual (axial) dipole moments for the period 5–120 Ma collected from the PINT database. The red circles are the VDMs obtained in the present study and the mean of it is represented as a blue circle. The open squares are mean VDM obtained from continental lava flows (Goguitchaichvili *et al.* 2002), diamonds are mean VADMs obtained from submarine basaltic glass (Tauxe and Staudigel 2004), and closed circle is mean VDM obtained from single plagioclase crystals of Rajmahal basalts (Tarduno *et al.* 2001). The red dashed horizontal line represents the strength of the present day (geomagnetic) field. The geomagnetic polarity timescale presented at the bottom of the figure is after Walker *et al.* (2012).

5.2 *Paleointensity variations with time*

Usual alternating field (AF) and thermal demagnetization techniques were used to determine paleomagnetic directions of RT and ST recently by Kapawar and Venkateshwarlu (2019, 2020). Their work suggested that most of the samples of RT and ST carry small VRM and after removal (either by using AF or thermal demagnetization) proposes a well-defined ChRM component of normal polarity. Before actual consideration of samples for PI study, the paleomagnetic results were assessed and only those samples were selected which are free from viscous and IRM components of magnetizations, for the reason that such samples may not provide reliable paleointensity data. The characteristic remanence magnetization (ChRM) directions were isolated by the principal component analysis (PCA) method (Kirschvink 1980).

The predominant dipolar nature of earth's magnetic field is well understood at least for the past 250 Ma (e.g., Bloxham 2000). The paleointensity estimations were obtained from the slope of Arai diagrams with described temperature ranges. The estimation of VDM in this study is from the formula devised by Perrin and Schnepp (2004) as follows:

$$\mathrm{VDM} = 4\pi R^3/2\mu o \cdot F(1 + 3\cos^2 I)^{1/2},$$

where, R is the radius of the Earth, F is paleointensity, and I is inclination (paleo-inclination). The inclination values used here are from Kapawar and Venkateshwarlu (2019, 2020). The VDM determined for the times ∼117 Ma from these rocks is 2.93×10^{22} Am^2 (blue circle in figure 6), which corresponds to ∼30% of the present axial dipole moment (∼8.0×10^{22} Am^2).

Commonly, obtaining a single paleointensity value from the sampling site (table 1) is not enough to express the paleointensity for a site, but the samples of this study satisfy all the defined criteria and are accepted. Those accepted specimens have demonstrated a linear trend on the Arai plot and have shown a lesser variation of susceptibility (figure 5). Therefore, the paleointensity data from these samples propose their suitability for further usefulness and are in some way can be used to model the convective processes in the Earth's core which have been responsible for generating the magnetic field (Juarez *et al.* 1998).

6. Conclusions

We present here new paleointensity results from whole-rock basalts of the Rajmahal–Sylhet Traps dated ∼117 Ma. They represent the main phase of the flood volcanism over the Indian Plate associated with the Kerguelen hotspot in the southern Indian Ocean. Our new mean paleointensity value of 17.20 ± 1.89 μT with a mean VDM of 2.93×10^{22} Am^2 when combined with other published data show a better agreement of low magnetic field intensities during the long CNS. Thus the present study establishes new results from the study area and suggests RT and ST basalts suitability for further more elaborative paleointensity studies. Our results are analogous with the data of Tanaka and Kono (2002) and Zhao *et al.* (2004) suggesting low field strength, and disagrees with the reports of Tarduno *et al.* (2001) and Tauxe (2006) suggesting the high magnetic field strength at this particular geologic time. Tauxe (2006) also stated that the average high dipole values obtained are resultant of polarity interval length and not probably used to find mean value. Also Juarez *et al.* (1998) quoted that the average dipole moment is substantially less than the present day value (∼8.0×10^{22} Am^2) and thus validates our results. To confirm the discrepancy in the reports (of high and low dipole values from the same geologic unit) and to assess the link between high reversal rates and lower field strengths, more robust paleointensity studies from the study area are needed.

Acknowledgements

We thank the Director of CSIR-NGRI, Hyderabad for the permission to publish this work (NGRI/LIB/2020/Pub-212). MRK is grateful to T Radhakrishna and K Deenadayalan for timely guidance. Authors thank anonymous reviewers for valuable comments and Munukutla Radhakrishna, Associate Editor for careful handling of the manuscript. MRK extend thanks to CSIR, India for SRF (P-81-101).

Author statement

M R Kapawar collected the samples, generated and processed the data, and wrote the original draft of the manuscript. Venkateshwarlu Mamilla conceptualized, supervised, and wrote the original draft of the manuscript. Both the authors reviewed, revised and approved the manuscript.

References

Baksi A K 1995 Petrogenesis and timing of volcanism in the Rajmahal flood basalt province, northeast India; *Chem. Geol.* **121** 73–90.

Baksi A K, Ray Barman T, Paul D K and Farrar E 1987 Widespread Early Cretaceous flood basalt volcanism in eastern India: Geochemical data from the Rajmahal–Bengal–Sylhet Traps; *Chem. Geol.* **63** 133–141.

Biggin A J and Paterson G A 2014 A new set of qualitative reliability criteria to aid inferences on palaeomagnetic dipole moment variations through geological time; *Front. Earth Sci.* **2** 24, https://doi.org/10.3389/feart.2014.00024.

Bloxham J 2000 Sensitivity of the geomagnetic axial dipole to thermal core-mantle interactions; *Nature* **405** 63–65.

Coe R, Hongre L and Glatzmaier G 2000 An examination of simulated geomagnetic reversals from a paleo-magnetic perspective; *Phil. Trans. Roy. Soc. London Ser. A* **357** 1787–1813.

Coffin M F, Pringle M S, Duncan R A, Gladczenko T P, Storey M, Muller R D and Gahagan L A 2002 Kerguelen hotspot magma output since 130 Ma; *J. Petrol.* **43(7)** 1121–1137, https://doi.org/10.1093/petrology/43.7.1121.

Cottrell R D and Tarduno J A 2000 In search of high-fidelity geomagnetic paleointensities: A comparison of single plagioclase crystal and whole rock Thellier-Thellier analyses; *J. Geophys. Res.* **105(B10)** 23579–23594, https://doi.org/10.1029/2000JB900219.

Day R, Fuller M and Schmidt V A 1977 Hysteresis properties of titanomagnetites: Grain-size and compositional dependence; *Phys. Earth Planet. Inter.* **13(4)** 260–267.

Dunlop D J 2002a Theory and application of the Day plot (Mrs/Ms versus Hcr/Hc). 1: Theoretical curves and tests using titanomagnetite data; *J. Geophys. Res.: Solid Earth* **107(B3)** EPM-4, https://doi.org/10.1029/2001JB000486.

Dunlop D J 2002b Theory and application of the Day plot (Mrs/Ms versus Hcr/Hc). 2: Application to data for rocks, sediments, and soils; *J. Geophys. Res.: Solid Earth* **107(B3)** EPM-5, https://doi.org/10.1029/2001JB000487.

Evans P 1964 The tectonic framework of Assam; *J. Geo. Soc. of India* **5** 80–96.

Ghatak A and Basu A R 2013 Isotopic and trace element geochemistry of alkalic–mafic–ultramafic–carbonatitic complexes and flood basalts in NE India: Origin in a heterogeneous Kerguelen plume; *Geochim. Cosmochim. Acta* **115** 46–72, https://doi.org/10.1016/j.gca.2013.04.004.

Glatzmaier G A, Coe R S, Hongre L and Roberts P H 1999 The role of the Earth's mantle in controlling the frequency of geomagnetic reversals; *Nature* **401** 885–890.

Goguitchaichvili A, Cejudo Ruiz R, Sanchez Bettucci L, Aguilar Reyes B, Alva-Valdivia L M, Urrutia-Fucugauchi J, Morales J and Calvo Rathert M 2008 New absolute paleointensity results from the Parana Magmatic Province (Uruguay) and the Early Cretaceous geomagnetic paleofield; *Geochem. Geophys. Geosyst.* **9** Q11008, https://doi.org/10.1029/2008GC002102.

Goguitchaichvili A, Urrutia-Fucugauchi J and Alva-Valdivia L 2002 Mesozoic dipole low: Myth or reality?; *Eos Trans. AGU* **83(41)** 457–461.

Juarez M T, Tauxe L, Gee J S and Pick T 1998 The intensity of the Earth's magnetic field over the past 160 million years; *Nature* **394** 878–881.

Kapawar M R and Venkateshwarlu M 2019 Rock magnetic and paleomagnetic investigations of Sylhet traps, Shillong Plateau, NE India; *J. Geodyn.* **127** 31–41, https://doi.org/10.1016/j.jog.2019.05.003.

Kapawar M R and Venkateshwarlu Mamilla 2020 Paleomagnetism and rock magnetism of early Cretaceous Rajmahal basalts, NE India: Implications for paleogeography of the Indian subcontinent and migration of the Kerguelen hotspot; *J. Asian Earth Sci.* **201** 104517, https://doi.org/10.1016/j.jseaes.2020.104517.

Kato C, Sato M, Yamamoto Y, Tsunakawa H and Kirschvink J 2018 Paleomagnetic studies on single crystals separated from the middle Cretaceous Iritono granite; *Earth Planets Space* **70** 176, https://doi.org/10.1186/s40623-018-0945-y.

Kent R W, Pringle M S, Muller R D, Saunders A D and Ghose N C 2002 $^{40}Ar/^{39}Ar$ geochronology of the Rajmahal basalts, India, and their relationship to the Kerguelen Plateau; *J. Petrol.* **43(7)** 1141–1153.

Kirschvink J L 1980 The least-squares line and plane and the analysis of palaeomagnetic data; *Geophys. J. Inter.* **62(3)** 699–718.

Leonhardt R 2006 Analyzing rock magnetic measurements: The RockMagAnalyzer 1.0 software; *Comput. Geosci.* **32** 1420–1431, https://doi.org/10.1016/j.cageo.2006.01.006.

Leonhardt R, Heunemann C and Krasa D 2004 Analysing absolute paleointensity deternations: Acceptance criteria and the software ThellierTool4.0; *Geochem. Geophys. Geosyst.* **5** Q12016, https://doi.org/10.1029/2004GC000807.

Loper D E and McCartney K 1986 Mantle plumes and the periodicity of magnetic field reversals; *Geophys. Res. Lett.* **13** 1525–1528.

Mena M, Goguitchaichvili A, Solano M C and Vilas J F 2011 Paleosecular variation and absolute geomagnetic paleointensity records retrieved from the Early Cretaceous Posadas Formation (Misiones, Argentina); *Stud. Geophys. Geod.* **55(2)** 279–309, https://doi.org/10.1007/s11200-011-0016-3.

Nagata T, Arai Y and Momose K 1963 Secular variation of the geomagnetic total force during the last 5000 years; *J. Geophys. Res.* **68(18)** 5277–5281.

Pan Y, Hill M, Zhu R and Shaw J 2004 Further evidence for low intensity of the geomagnetic field during the early Cretaceous time: Using the modified Shaw method and microwave technique; *Geophys. J. Inter.* **157** 553–564, https://doi.org/10.1111/j.1365246X.2004.02253.x.

Perrin M and Schnepp E 2004 IAGA paleointensity database: Distribution and quality of the data set; *Phys. Earth Planet. Inter.* **147(2–3)** 255–267, https://doi.org/10.1016/j.pepi.2004.06.005.

Perrin M and Shcherbakov V 1997 Paleointensity of the Earth's magnetic field for the past 400 Ma: Evidence for a dipole structure during the Mesozoic low; *J. Geomag. Geoelectr.* **49** 601–614.

Pick T and Tauxe L 1993 Geomagnetic palaeointensities during the Cretaceous normal superchron measured using submarine basaltic glass; *Nature* **366** 238–242.

Prevot M, Derder M, McWilliams M M and Thompson J 1990 Intensity of the Earth's magnetic field: Evidence for a Mesozoic dipole low; *Earth Planet. Sci. Lett.* **97** 129–139.

Prevot M, Mankinen E A, Coe R S and Gromme C S 1985 The Steens Mountain (Oregon) geomagnetic polarity transition: 2. Field intensity variations and discussion of reversal models; *J. Geophys. Res.* **90(B12)** 10417–10448, https://doi.org/10.1029/JB090iB12p10417.

Qin H, He H, Liu Q and Cai S 2011 Palaeointensity just at the onset of the Cretaceous normal superchron; *Phys. Earth Planet. Int.* **187** 199–211, https://doi.org/10.1016/j.pepi.2011.05.009.

Ray J S, Pattanayak S K and Pande K 2005 Rapid emplacement of the Kerguelen plume-related Sylhet Traps, eastern India: Evidence from ^{40}Ar–^{39}Ar geochronology; *Geophys. Res. Lett.* **32(10)** L10303, https://doi.org/10.1029/2005GL022586.

Sakai H, Funaki M, Sato T, Rao K V, Takigami Y, Sakai H A and Hirooka K 1997 Paleomagnetic study of the Rajmahal trap in India. Discussion of geomagnetic dipole moment and reconstruction of Gondwanaland; *Proc NIPR Symp. Antarct. Geosci.* **10** 68–78.

Sarkar A, Datta A K, Poddar B C, Bhattacharyya B K, Kollapuri V K and Sanwal R 1996 Geochronological studies of Mesozoic igneous rocks from eastern India; *J. Southeast Asian Earth Sci.* **13(2)** 77–81.

Selkin P A and Tauxe L 2000 Long-term variations in palaeointensity; *Phil. Trans. Roy. Soc. London Ser. A* **555** 1065–1088, https://doi.org/10.1098/rsta.2000.0574.

Sherwood G J, Baer G and Mallik S B 1993 The strength of the geomagnetic field during the Cretaceous Quiet Zone: Palaeointensity results from Israeli and Indian lavas; *J. Geomagn. Geoelect.* **45** 339–360.

Talukdar S C and Murthy M V N 1971 The Sylhet Traps, their tectonic history, and their bearing on problems of Indian flood basalt provinces; *Bull. Volcanol.* **35(3)** 602–618.

Tanaka H and Kono M 2002 Paleointensities from a Cretaceous basalt platform in Inner Mongolia, northeastern China; *Phys. Earth Planet. Inter.* **133(1–4)** 147–157.

Tanaka H, Kono M and Uchimura H 1995 Some global features of paleointensity in geological time; *Geophys. J. Int.* **120** 97–102.

Tarduno J A and Smirnov A V 2001 Stability of the Earth with respect to the spin axis for the last 130 million years; *Earth Planet. Sci. Lett.* **184** 549–553, https://doi.org/10.1016/S0012-821X(00)00348-4.

Tarduno J A, Cottrell R D and Smirnov A V 2001 High geomagnetic intensity during the Mid-Cretaceous from Thellier analyses of single plagioclase crystals; *Science* **291** 779–1783, https://doi.org/10.1126/science.1057519.

Tarduno J A, Cottrell R D and Smirnov A V 2002 The Cretaceous superchrongeodynamo observations near the tangent cylinder; *Proc. Nat. Acad. Sci.* **99** 14020–14025, https://doi.org/10.1073/pnas.222373499.

Tarduno J A, Cottrell R D and Smirnov A V 2007 Paleointensity: Absolute determinations using single plagioclase crystals; In: *Encyclopedia of Geomagnetism and Paleomagnetism* (eds) Gubbins D and Herrero-Bervera E, Springer, Dordrecht, https://doi.org/10.1007/978-1-4020-4423-6_251.

Tauxe L 2006 Long-term trends in paleointensity: The contribution of DSDP/ODP submarine basaltic glass collections; *Phys. Earth Planet. Inter.* **156(3–4)** 223–241, https://doi.org/10.1016/j.pepi.2005.03.022.

Tauxe L and Staudigel H 2004 Strength of the geomagnetic field in the Cretaceous Normal Superchron: New data from submarine basaltic glass of the Troodos Ophiolite; *Geochem. Geophys. Geosyst.* **5** Q02H06, https://doi.org/10.1029/2003GC000635.

Thellier E and Thellier O 1959 Sur l'intensite du champ magnetique terrestre dans le passe historique et geologique; *Ann. Geophys.* **15** 285–376.

Walker J D, Geissman J W, Bowring S A, Babcock L E and Compilers 2012 Geologic Time Scale 4.0; *Geol. Soc. Am.*, https://doi.org/10.1130/2012.CTS004R3C.

Yu Y L and Tauxe L 2005 Testing the IZZI protocol of geomagnetic field intensity determination; *Geochem. Geophys. Geosyst.* **6** Q05H17, https://doi.org/10.1029/2004GC000840.

Yu Y, Tauxe L and Genevey A 2004 Towards an optimal geomagnetic field intensity determination technique; *Geochem. Geophys. Geosyst.* **5** Q02H07, https://doi.org/10.1029/2003GC000630.

Zhao X, Riisager P, Riisager J, Draeger U, Coe R S and Zheng Z 2004 New palaeointensity results from Cretaceous basalt of Inner Mongolia China; *Phys. Earth Planet. Inter.* **141(2)** 131–140, https://doi.org/10.1016/j.pepi.2003.12.003.

Zhu R, Hoffman K A, Pan Y, Shi R and Li D 2003 Evidence for weak geomagnetic field intensity prior to the Cretaceous normal superchron; *Phys. Earth Planet. Inter.* **136(3)** 187–199, https://doi.org/10.1016/S0031-9201(03)00034-7.

Zhu R, Lo C H, Shi R, Shi G, Pan Y J and Shao J 2004 Palaeointensities determined from the middle Cretaceous basalt in Liaoning Province, northeastern China; *Phys. Earth Planet. Inter.* **142(1)** 49–59, https://doi.org/10.1016/j.pepi.2003.12.013.

Zhu R, Pan Y, Shaw J, Li D and Li Q 2001 Geomagnetic palaeointensity just prior to the Cretaceous normal superchron; *Phys. Earth Planet. Inter.* **128(1–4)** 207–222, https://doi.org/10.1016/S0031-9201(01)00287-4.

Corresponding editor: Munukutla Radhakrishna